

Synthesis, characterization of Ag/MCM-41 and the catalytic performance for liquid-phase oxidation of cyclohexane

Hong Zhao^a, Jicheng Zhou^{a,*}, Hean Luo^a, Chuyi Zeng^{a,b}, Dehua Li^a, and Yuejin Liu^a

^aDepartment of Chemical Engineering, Xiangtan University, Hunan 411105, P.R. China

^bDepartment of Chemical Engineering, Tsinghua University, Beijing 100084, P.R. China

Received 23 October 2005; accepted 14 January 2006

Nano-scale silver supported mesoporous molecular sieve Ag/MCM-41 was directly prepared by one-pot synthesis method. The prepared sample was characterized by XRD, TEM, and N₂ sorption. The results showed that the sample of Ag/MCM-41 had no appreciable incorporation of silver into the mesoporous matrix of MCM-41 with good crystallinity, and silver nanoparticles were dispersed inside or outside of the channels in the mesoporous host. The catalytic performance of the sample for the cyclohexane liquid-phase oxidation into cyclohexanone and cyclohexanol by oxygen in the absence of solvents without inducing agents was investigated. The 83.4% selectivity to cyclohexanol and cyclohexanone at 10.7% conversion of cyclohexane was obtained over Ag/MCM-41 catalyst at 428 K for 3 h. The turn over numbers (TONs) of Ag/MCM-41 was up to 2946. The catalytic activity of Ag/MCM-41 was also compared with Ag/TS-1 as well as Ag/Al₂O₃. The results indicated that Ag/MCM-41 showed superior activity to both Ag/TS-1 and Ag/Al₂O₃. A calcined Ag/MCM-41 was found to be an efficient catalyst for the cyclohexane oxidation into cyclohexanol and cyclohexanone using oxygen as oxidant.

KEY WORDS: mesoporous molecular sieves; nanostructured silver; cyclohexane; oxidation.

1. Introduction

The oxidation of cyclohexane is an industrially important chemical reaction for the manufacture of caprolactam, nylon and other products. The present industrial process for cyclohexane oxidation is widely carried out around 423 K and 1–2 MPa pressure employed metal cobalt salt or metal-boric acid as homogeneous catalyst. The cyclohexane conversion is always controlled about 4% to keep 70–85% selectivity to cyclohexanol and cyclohexanone. In recent years, many attempts have been made to improve or substitute the classical process by developing heterogeneous catalysts with oxygen or peroxides as nonpolluting oxidants under the mild conditions [1–9]. However, owing to low efficiency of peroxides that make the value of the oxidant higher than that of the product [10], further emphasis is given on the catalytic oxidation in liquid phase with the cheaper oxygen as oxidant [11]. Using molecular oxygen as oxidant, some transitional metals such as Ti, V, Cr, Co, Mn, Fe, Mo, Au and metal oxides contained in or on various supports have been extensively studied as the cyclohexane oxidation catalyst [12–18]. Up to now, the development of new heterogeneous catalysts for the oxidation of cyclohexane is still of considerable commercial and academic interest [10].

Silver is always used to catalyze some oxidation reactions with outstanding activity, such as methanol

oxidation [19], the partial epoxidation of ethylene, propylene and other low hydrocarbons [20–23]. Since Haruta and co-workers discovered the excellent catalysis of gold nanoparticles in the oxygen-transfer reactions near ambient temperature [24], nanostructured silver also has attracted great interest [25–28]. It has been proved that supported silver catalysts possess a stable activity for CO oxidation at low temperatures [29] and nano-silver particles on the outer surface of the zeolite can accelerate the SCR reaction apparently which provide strong adsorption centers for NO_x [30]. However, silver has rarely been considered as a catalyst for saturated hydrocarbons selective oxidation. Especially, there is no report related to the catalytic performance for the cyclohexane liquid-phase oxidation of Ag/MCM-41. In this investigation, we have directly prepared nano-scale silver supported mesoporous molecular sieve Ag/MCM-41 by one-pot synthesis method. The catalytic performance of the sample for the cyclohexane liquid-phase oxidation into cyclohexanone and cyclohexanol by oxygen in the absence of solvents without inducing agents is also investigated.

2. Experimental

2.1. Sample preparation

About 1 wt.% Ag catalyst was synthesized as follows. 2.28 g of hexadecyltrimethylammonium bromide (CTAB) was dissolved in 25 mL deionized water. When

* To whom correspondence should be addressed.
E-mail: zhoujicheng@sohu.com

the mixture became clear under magnetic stirring, an aqueous solution of AgNO_3 (0.1 mol/L, 1.39 mL) was added dropwise over a period of 20 min. Then 6 mL NaBH_4 solution (0.1 mol/L) was added to form a brown solution. 5.28 g of tetraethylorthosilicate (TEOS) was added dropwise to the brown solution and then 2 mL aqueous solution of NaOH (25 wt.%) was introduced to the Ag/surfactant solution. After vigorously stirred for 2 h, the pH of the mixture was adjusted to about 10.5 using HCl solution (37 wt.%), then the precipitation of a light yellow gel was formed. The gel solution was then transferred to a Teflon bottle and heated under static conditions at 383 K for 2–3 days. The precipitate was then filtered, washed several times with deionized water and ethanol respectively, dried overnight at room. After calcined in air at 823 K for 5 h to remove template, the yellowy-gray Ag/MCM-41 sample was obtained. Molar composition of the synthesis gel for Ag/MCM-41 samples was: SiO_2 : C_{16}TAB : Na_2O : H_2O : $\text{Ag}(\text{NO}_3)_2$ = 1: 0.25: 0.24: 100–200: 0–0.01.

2.2. Characteristics of catalysts

The powder X-ray diffraction patterns are recorded on a Rigaku D/max-RB diffractometer using 120 mA nickel-filtered $\text{CuK}\alpha$ radiations ($\lambda = 1.5418 \text{ \AA}$) at a voltage of 45 kV with a step size of 0.002. The d_{100} values are obtained using the Bragg diffraction equation. The distance between the pore centers of the hexagonal structure is calculated from the relation, $a_0 = 2d_{100}/3^{0.5}$. N_2 adsorption and desorption isotherms are obtained at 77.25 K on a Micromeritics ASAP-2010 system. HRTEM images and electron diffraction (EDS) patterns are performed on a JEM-2010F microscope operated at 200 kV.

2.3. Catalytic experiments

Catalytic reactions were performed in a 50 mL autoclave reactor with a Teflon insert inside. Typically, 8.4 g cyclohexane and 0.042 g catalyst were placed in the reactor. After heated to expected temperature under stirring, the reactor was charged 1.4 MPa O_2 for 3 h continuously. When the reaction was finished, the liquid was extracted from the autoclave and the catalyst was separated. Cyclohexanol and cyclohexanone were analyzed by GC equipped with an AC-10 capillary column (0.32 mm \times 30 m) and an FID detector. Chlorobenzene was used as an internal standard. The conversion was calculated based on the starting cyclohexane. Cyclohexyl hydroperoxide (CHHP) concentration was determined by iodometric titration. Acid and ester are determined by acid-base titration.

3. Results and discussion

Figure 1(a) shows low angle X-ray diffraction patterns of the calcined porous silica host and the calcined

doped sample with 1.0 wt.% Ag. The peak appearing at low angle ($2\theta = 2.6$) corresponds to (100) plane of MCM-41 indicating ordered pore structure of MCM-41, which suggests that the hexagonal pore structure of MCM-41 should be retained after being incorporated with Ag. However, the fact that peak intensity for the low-angle reflections decreases in sample Ag/MCM-41 shows that the formation of Ag clusters inside the channels leads to the loss of ordered structure, which is consistent with the reports in literature [26]. The average unit cell parameter (a_0) is summarized in table 1. In general, the incorporation of a larger cation, such as Ag(I) (1.26 \AA), in tetrahedral geometry for Si(IV) (0.40 \AA) is expected to increase the lattice parameter significantly. However, as shown in table 1, only a small increase in the lattice constant is noticed compared with corresponding Ag-free MCM-41. The result indicates that there is no appreciable incorporation of silver into the mesoporous matrix [31]. The observed slight expansion in a_0 values and shifting of the reflections to the lower 2θ values could be explained by that silver

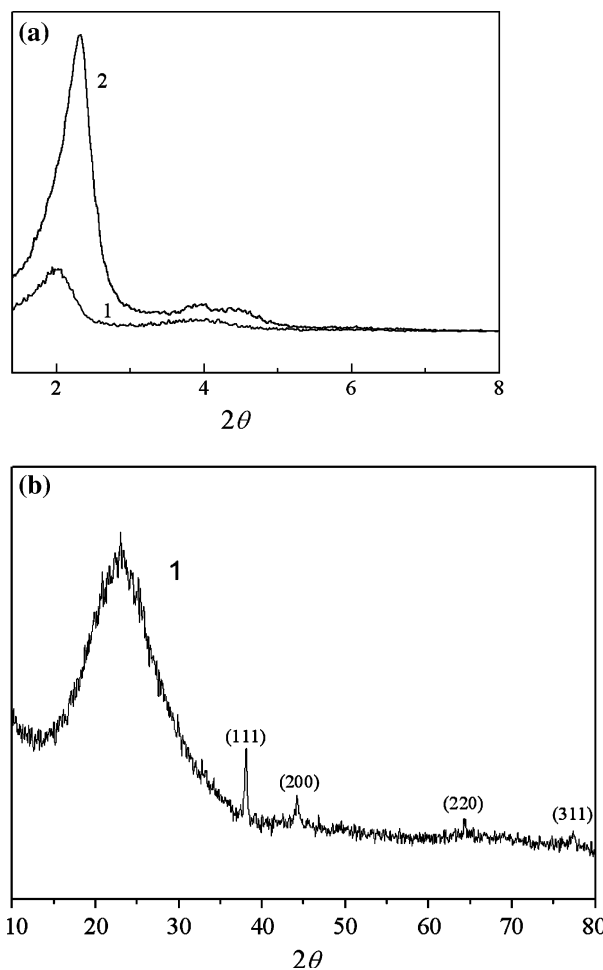


Figure 1. (a) SAXRD patterns and (b) XRD patterns of Ag/MCM-41(1) and MCM-41(2).

Table 1
Textural properties obtained from XRD and N₂ physisorption

Sample	d_{100} (nm)	a_0^a (nm)	S_{BET} (m ² /g)	V_{BJH}^b (cm ³ /g)	D_{BJH}^b (nm)
MCM-41	3.81	4.40	1099	1.14	2.71
Ag/MCM-41	3.92	4.53	987.1	1.00	2.87

^a $a_0 = 2d_{100}/(3)^{1/2}$.

^b Calculated from the desorption branch of the nitrogen adsorption and desorption isotherms.

species is filled the pores of MCM-41, which slightly deform the matrix. High angle X-ray diffraction pattern ($2\theta = 10\text{--}80$), figure 1(b), shows well-resolved peaks around 38.0° , 44.3° , 64.4° , and 77.6° , which are respectively corresponding to (111), (200), (220), and (311) planes of the cubic structure of silver with lattice constant of $a = 4.09$.

3.1. HRTEM images

The HRTEM image of the calcined Ag/MCM-41 sample is shown in figure 2(a), while the inset is the filtered image (b). In agreement with the above SAXRD results, the synthesized sample is of hexagonal meso-structure and remains intact after supported with Ag [32]. The simultaneous EDS analysis, as shown in

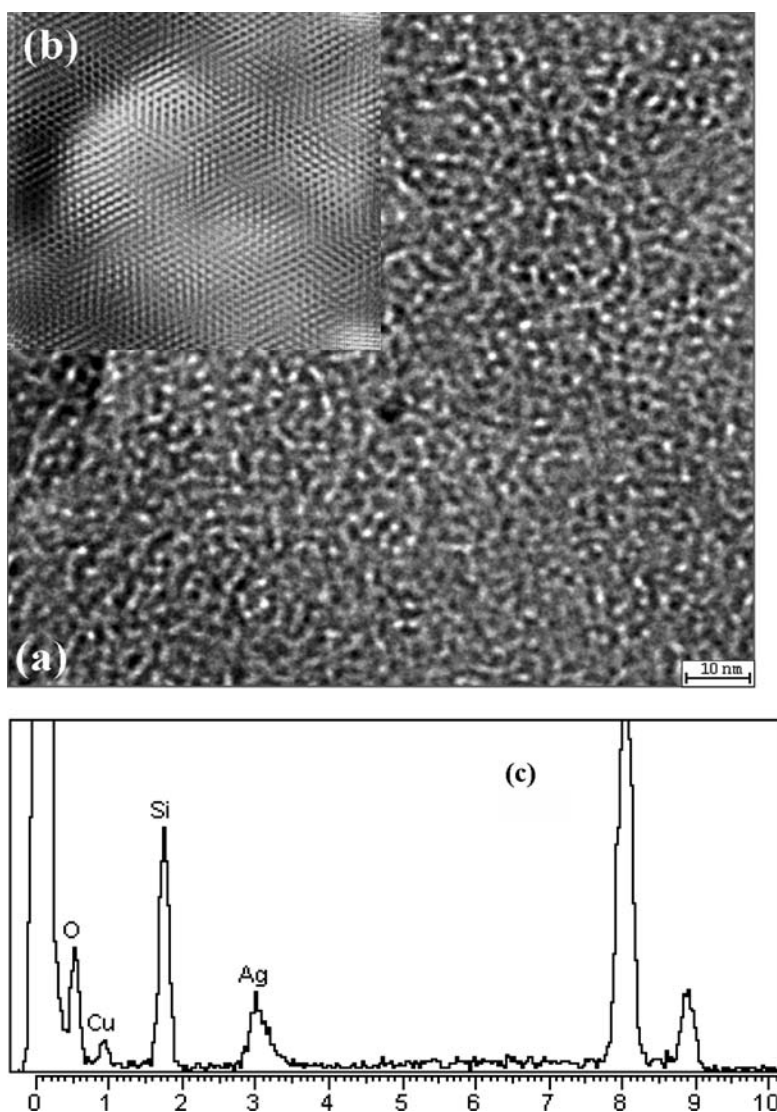


Figure 2. Representative HRTEM images of Ag/MCM-41 sample. (a) The HRTEM images of the calcined Ag/MCM-41, (b) The simultaneous filtered image, (c) The simultaneous EDS spectrum.

figure 2(c), indicates that Ag element exists on the mesoporous host.

3.2. N_2 sorption isotherms

Figure 3 presents the N_2 adsorption/desorption isotherm of the Ag/MCM-41 sample. The sample exhibits a typical adsorption curve of type IV, which is the characteristic of nanostructured materials with uniform mesopores. The adsorption and desorption isotherm shows a large increase in the relative pressure (P/P_0) range from 0.3 to 0.4, which is due to the capillary condensation of nitrogen within the mesopores. The sharpness of the inflection step reflects the uniform pore size distribution of the Ag/MCM-41 sample [33]. In consonance with results of XRD, the N_2 adsorption/desorption isotherm also confirm that the Ag/MCM-41 sample possess high structural integrity.

3.3. Catalytic activity

The results of cyclohexane catalytic aerobic oxidation using the above catalyst are listed in table 2, together with the silver content and turn over numbers (TONs), which are compared with Ag/TS-1 and Ag/ Al_2O_3 carried out under the same reaction conditions. Blank experiments demonstrate that catalyst is necessary for the cyclohexane oxidation to proceed significantly without any additive, since little products are detected when the reaction is attempted for as long as 3 h at 413 K without the silver catalyst. In comparison with Ag/TS-1 and Ag/ Al_2O_3 , Ag/MCM-41 shows higher TONs and cyclohexane conversion and better selectivity to cyclohexanone and cyclohexanol under the same reaction conditions. The results indicate that similar to nanostructured gold catalysts, supports have effect on the activity of nanostructured silver catalysts [24]. Table 2 also shows that the lower silver content Ag/MCM-41 has the slightly higher conversion but remarkably lower selectivity to cyclohexanol and

cyclohexanone. One of the possible reasons may be attributed to that the silver particles of the Ag/MCM-41 sample with lower silver content are smaller, since smaller silver particles have stronger surface energy, which will lead to the overreaction of cyclohexanol and cyclohexanone to by-products.

Figure 4 shows the effect of reaction time on the oxidation reaction of cyclohexane at 413 K over Ag/MCM-41(0.25). It can be seen that the cyclohexane conversion steadily increased with increasing reaction time. In addition, at initial 2 h, the distributions of cyclohexanol and cyclohexanone are almost equal, but with further increasing reaction time, the cyclohexanol selectivity decreases while the selectivity to cyclohexanone rises to the maximum 47.9% at 4 h, and then reduces substantially. The distribution of CHHP decreases during the all reaction period. At initial 2 h CHHP is one of the major products with a selectivity of 31.6% and at 6 h the amount of CHHP became little (<5%). On the other hand, the distribution of by-products that are composed of acids and esters increases with increasing reaction time. This result indicates that the rate of oxidizing the cyclohexane was slower than that of oxidizing cyclohexanol and cyclohexanone when the cyclohexanol and cyclohexanone concentration is higher. Therefore, the proper reaction time is 3–4 h.

Figure 5 shows the effect of reaction temperature on the oxidation reaction of cyclohexane at reaction time of 3 h over Ag/MCM-41(0.5). The conversion increases slowly until 408 K (cyclohexane conversion 5.5%) beyond which a sharp increase occurs until 428 K (cyclohexane conversion 10.7%). When the reaction temperature goes beyond this value, the cyclohexane conversion changes slightly, but the conversion toward the desired cyclohexanol and cyclohexanone products decreases substantially.

The dependence of the selectivity with the temperature is also shown in figure 5. At lower temperature, besides the desired cyclohexanol and cyclohexanone products, a mass of CHHP exists with the maximum selectivity of 36.2%. With the increase of the temperature, the cyclohexanol and cyclohexanone selectivity increases while the CHHP selectivity decreases sharply. When the temperature goes beyond 418 K, only very small quantity of CHHP can be detected in the reaction mixture (<0.5%). On the other hand, the selectivity to cyclohexanol and cyclohexanone increases with the temperature until reaching the maximum of 45.3% and 38.1% respectively at 428 K, and then decrease with further increasing of temperature.

From the figures 4 and 5, we can see that the distribution of CHHP decreases accompanying the increasing of the cyclohexanol and cyclohexanone selectivity. This change tendency shows that CHHP is an important intermediate to decompose to cyclohexanol and cyclohexanone in this reaction. Combined with the fact that the reaction is terminated by the addition of 5 wt%

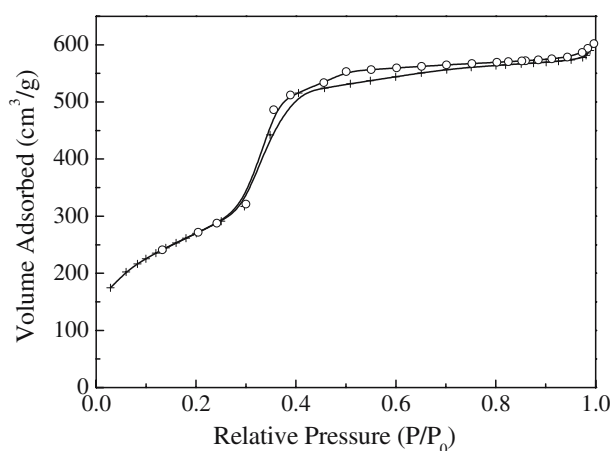


Figure 3. N_2 sorption isotherms for Ag/MCM-41 sample.

Table 2
Cyclohexane oxidation over Ag/MCM-41 catalyst^a

Catalyst	Ag content ^b (wt.%)	TON	Cov. (%)	Product selectivity (%) ^c			
				K	A	CHHP	Others
Blank	—	—	1.83	33.9	12.0	54.1	0
Ag/MCM-41(0.25)	0.25	2946	8.6	43.6	24.4	17.0	14.8
Ag/MCM-41(0.5) ^d	0.5	1834	10.7	45.3	38.1	0	16.6
Ag/MCM-41(0.5)	0.5	1437	8.4	37.2	26.3	26.3	10.3
Ag/TS-1(0.5) ^e	0.5	1044	6.1	32.3	16.7	40.0	10.8
Ag/Al ₂ O ₃ (0.5) ^e	0.5	416	2.7	15.1	10.3	74.6	0

^a Cyclohexane 0.1 mol, catalyst 0.042 g, O₂ 1.4 Mpa, 413 K, stirrer, reaction time 3h.

^b Accounted by the added amount in synthesis.

^c K: cyclohexanone; A: cyclohexanol, CHHP: cyclohexyl hydroperoxide, Others: acid and ester.

^d Reaction temperature was 428 K.

^e Prepared by precipitation method.

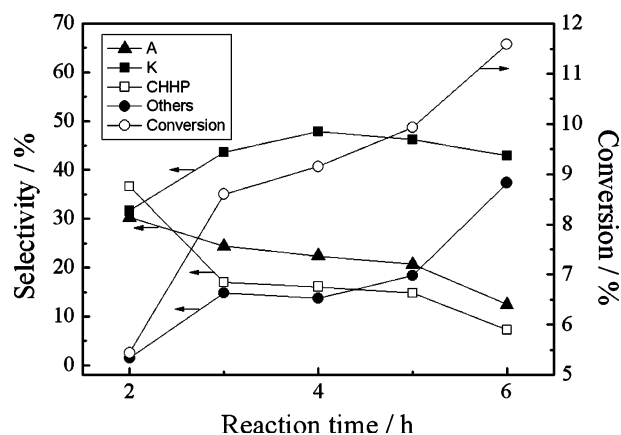


Figure 4. Reaction time dependence of the conversion and selectivity using Ag/MCM-41(0.25).

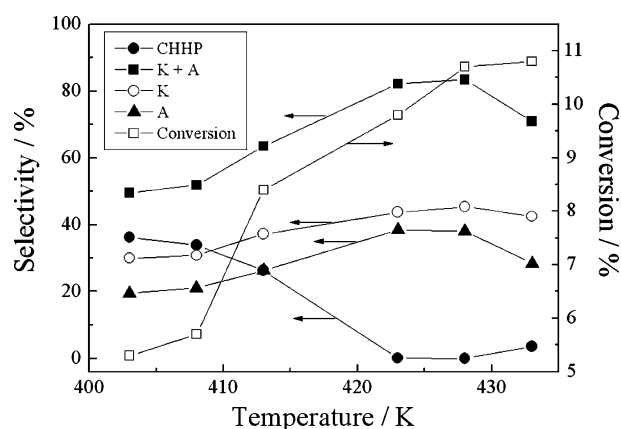


Figure 5. Reaction temperature dependence of the conversion and selectivity using Ag/MCM-41(0.5).

2,6-di-tertbutyl-4-methylphenol, the oxidation of cyclohexane should be believed to be a free-radical mechanism.

4. Conclusions

Nano-scale silver supported mesoporous molecular sieve Ag/MCM-41 was directly prepared by one-pot synthesis method using hexadecyltrimethylammonium bromide (CTAB) as both a stabilizing agent for Ag nanoparticles and a template for MCM-41 host. XRD result shows that there was no appreciable incorporation of silver into the mesoporous matrix, silver nanoparticles present inside the channels or deposits on the external surface of MCM-41.

Ag/MCM-41 is found to be an effective catalyst for the cyclohexane oxidation to cyclohexanol and cyclohexanone using molecular oxygen as oxidant in the absence of solvents. Compared with Ag/TS-1 and Ag/Al₂O₃, Ag/MCM-41 shows higher turnover number and better cyclohexanone and cyclohexanol selectivity. The turn over numbers (TONs) of Ag/MCM-41 can be up to 2946. The conversion of cyclohexane is up to 10.7%, selectivity to cyclohexanol and cyclohexanone are 83.4% at 428 K for 3 h. The experiment results suggest that the oxidation of cyclohexane be a free-radical mechanism using Ag/MCM-41 as catalyst.

Acknowledgments

The authors are grateful to the R&D Foundation of China Petroleum & Chemical Corporation (No. 205054)

References

- [1] F.A. Chavez, C.V. Nguyen, M.M. Olmstead and P.K. Maschak, *Inorg. Chem.* 35 (1996) 6282.
- [2] J.M. Thomas, R. Raja, G. Sankar and R.G. Bell, *Acc. Chem. Res.* 34 (2001) 191.
- [3] R. Raja, G. Sankar and J.M. Thomas, *J. Am. Chem. Soc.* 121 (1999) 11926.

- [4] N. Mizuno, C. Nozaki, I. Kiyoto and M. Misono, *J. Am. Chem. Soc.* 120 (1998) 9267.
- [5] A. Maldotti, C. Bartocci, G. Varani, A. Molinari, P. Battioni and D. Mansuy, *Inorg. Chem.* 35 (1996) 1126.
- [6] B.C. Bales, P. Brown, A. Dehestani and J.M. Mayer, *J. Am. Chem. Soc.* 127 (2005) 2832.
- [7] B. Moden, L. Oliviero, J. Dakka, J.G. Santiesteban and E. Iglesia, *J. Phys. Chem. B* 108 (2004) 5552.
- [8] C.C. Guo, G. Huang, D.C. Guo and X.B. Zhang, *Appl. Catal. A: Gen.* 247 (2003) 261.
- [9] J. Kaizer, E.J. Klinker, N.Y. Oh, J.-U. Rohde, W.J. Song, A. Stubna, J. Kim, E. Munck, W. Nam and L. Que Jr., *J. Am. Chem. Soc.* 126 (2004) 472.
- [10] U. Schuchardt, D. Cardoso, R. Sercheli, R. Pereira, R.S. da Cruz, M.C. Guerreiro, D. Mandelli, E.V. Spinacé and E.L. Pires, *Appl. Catal. A: Gen.* 211 (2001) 1.
- [11] J.R. Chen, H.H. Yang and C.H. Wu, *Org. Process. Res. Dev.* 8 (2004) 252.
- [12] P. Selvam and S.E. Dapurkar, *Appl. Catal. A: Gen.* 276 (2004) 257.
- [13] R. Zhao, D. Ji, G.M. Lv, G. Qian, L. Yan, X.L. Wang and J.S. Suo, *Chem. Commun.* (2004) 904.
- [14] L.P. Zhou, J. Xu, H. Miao, F. Wang and X.Q. Li, *Appl. Catal. A: Gen.* 292 (2005) 223.
- [15] J.H. Tong, Z. Li and C.G. Xia, *J. Mol. Catal. A: Chem.* 231 (2005) 197.
- [16] M.J.L. Kishore, G.S. Mishra and A. Kumar, *J. Mol. Catal. A: Chem.* 230 (2005) 35.
- [17] P. Tian, Z.M. Liu, Z.B. Wu, L. Xu and Y.L. He, *Catal. Today* 93–95 (2004) 735.
- [18] P. Selvam and S.E. Dapurkar, *J. Catal.* 229 (2005) 64.
- [19] G. Reuss, W. Disteldorf, O. Grundler and A. Hilt, in: *Ullmann's Encyclopedia of Industrial Chemistry*, 5th ed., Vol. A11, (VCH, Weinheim, 1988) p. 619.
- [20] Y.C. Kim, N.C. Park, J.S. Shin, S.R. Lee, Y.J. Lee and D.J. Moon, *Catal. Today* 87 (2003) 153.
- [21] T. Furusawa, L. Lefferts, K. Seshan and K. Aika, *Appl. Catal. B: Environ.* 42 (2003) 25.
- [22] X.W. Guo, R.P. Wang, X.S. Wang and J.Q. Hao, *Catal. Today* 93–95 (2004) 211.
- [23] V.M. Belousov, M. Vasiliev, N.Yu. Vilkova, O.P. Hryshchenko and B.E. Nieuwenhuys, *Appl. Catal. A: Gen.* 236 (2002) 245.
- [24] G.J. Hutchings and M. Haruta, *Appl. Catal. A: Gen.* 291 (2005) 2.
- [25] M.H. Huang, A. Choudrey and P. Yang, *Chem. Commun.* (2000) 1063.
- [26] X.G. Zhao, J.L. Shi, B. Hu, L.X. Zhang and Z.L. Hua, *Mater. Lett.* 58 (2004) 2152.
- [27] P.V. Adhyapaka, P. Karandikarb, K. Vijayamohanab, A.A. Athawalec and A.J. Chandwadkar, *Mater. Lett.* 58 (2004) 1168.
- [28] A.Q. Wang, J.H. Liu, S.D. Lin, T.S. Lin and Ch.Y. Mou, *J. Catal.* 233 (2005) 186.
- [29] Z.P. Qu, M.J. Cheng, W.X. Huang and X.H. Bao, *J. Catal.* 229 (2005) 446.
- [30] C. Shia, M.J. Cheng, Z.P. Qua, X.F. Yang and X.H. Bao, *Catal.* 36 (2005) 446.
- [31] A. Sakthivel and P. Selvam, *J. Catal.* 211 (2002) 134.
- [32] S.L. Gonza'lez-Corte's, T.C. Xiao, H.A. Al-Megren, L. Ruiz-González, N. Rees, I. Hannus, D. Méhn, J. Li and M.L.H. Green, *Mater. Res. Bull.* 40 (2005) 1112.
- [33] P.B. Amama, S. Lim, D. Ciuparu, L. Pfefferle and G.L. Haller et al., *Micropor. Mesopor. Mater.* 81 ((2005)) 191.